University of Baghdad
College of Engineering
JE
JOURNAL OF ENGINEERING

Journal of Engineering
journal homepage: www.joe.uobaghdad.edu.iq
Number 8 Volume 26 August 2020

Water Resources and Surveying Engineering

Salt Distribution in a Soil Irrigated by Subsurface Emitter

Ali Raheem Waseen
Engineer
Ministry of Water Resource
Baghdad - Iraq
E-mail: alirahim78engineer@gmail.com

Dr. Maysoon Basheer Abid*
Assis. Prof.
College of Engineering-University of Baghdad
Baghdad - Iraq
E-mail: maysoon basheer @coeng.uobagdad.edu.iq

ABSTRACT

The best design of subsurface trickle irrigation systems requires knowledge of water and salt distribution patterns around the emitters that match the root extraction and minimize water losses. The transient distribution of water and salt in a two-dimensional homogeneous Iraqi soil domain under subsurface trickle irrigation with different settings of an emitter is investigated numerically using 2D-HYDRUS software. Three types of Iraqi soil were selected. The effect of altering different values of water application rate and initial soil water content was investigated in the developed model. The coefficient of correlation (R^2) and the root-mean-square error (RMSE) was used to validate the predicted numerical result. This statistical analysis revealed that there was no much difference between the predicted numerical results, and the measured values. R^2 varied from 0.75 to 0.93 and the (RMSE) from 0.079 to 0.116. The comparison confirms the accuracy of the developed model, and it shows that it can be used to simulate the front wetting patterns of water and salt distribution under subsurface trickle irrigation systems. The simulation outcome showed that as the distance from the emitter increased, soil salinity far from the emitter decreased. As expected, irrigation duration and amount affects the dimension of the solute distribution.

Keywords: Hydrus 2D, subsurface emitter, salt distribution, soil moisture content.

توزيع الملح في تربة مروية بواسطة منقط تحت السطح

علي رحيم وسين
مهندس
وزارة الموارد المائية

د. ميسون بشير عبد
استاذ مساعد
كلية الهندسة – جامعة بغداد

الخلاصة

يتطلب أفضل تصميم لأنظمة الري بالتنقيط تحت سطح الأرض معرفة أنماط توزيع المياه والملح حول المنقطات التي تتوافق مع استخراج الجذر وتقلل من فقد المياه إلى أدنى حد. يتم دراسة التوزيع العابر للمياه والملح في منطقة تربة عراقية ثنائية

*Corresponding author
Peer review under the responsibility of University of Baghdad.
https://doi.org/10.31026/j.eng.2020.08.06

Article received: 1/2/2020
Article accepted:25/3/2020
Article published:1/8/2020

الأبعاد متجانسة تحت الري بالتنقيط تحت سطح الأرض مع بيئة مختلفة من المنقطات عدديًا باستخدام برنامج 2D HYDRUS. تم اختيار ثلاثة أنواع من التربة العراقية. تم دراسة تأثير تغيير القيم المختلفة لمعدل استخدام المياه والمحتوى الرطوبي الأولي لمياه التربة في النموذج المطور. تم استخدام معامل الارتباط (R^2) وخطأ الجذر التربيعي المربع (RMSE) للتحقق من صحة النتيجة العددية المتوقعة. أظهر التحليل الإحصائي أنه لا يوجد فرق كبير بين النتائج العددية المتوقعة والقيم المقاسة ، حيث تراوحت (R^2) من 0.75 إلى 0.93 و (RMSE) من 0.079 إلى 0.116. تؤكد المقارنة دقة النموذج المطوّر وتوضح أنه يمكن استخدامه لمحاكاة أنماط الترطيب الأمامية لتوزيع المياه والملح تحت أنظمة الري بالتنقيط تحت السطح.أظهرت نتائج المحاكاة أنه كلما زادت المسافة من المنقط ، انخفضت ملوحة التربة البعيدة عنه. كما هو متوقع ، تؤثر مدة وكمية الري على أبعاد وتوزيع المذاب.

1. INTRODUCTION

Subsurface trickle irrigation system is increasingly used in regions with limited water resources to irrigate crops. The best design of subsurface trickle irrigation systems requires knowledge of soil salt and water distribution patterns around the emitters that match the root extraction and minimize water losses. Numerical models can be used to simulate the transport of solutes and the flow of water in the subsurface. HYDRUS-2D software is considered a useful tool for simulating water flow and salt distribution under drip irrigation. The model numerically solves the Richards governing equation in two-dimensional coordinates for variably – saturated soil water flow and convection dispersion equation for solute transport. Several studies have been conducted on soil water with salt allocation beneath subsurface drip irrigation (SDI) with saline irrigation water. **(Roberts, et al., 2009)** used the HYDRUS-2D model to predict pattern salt accumulation from an SDI system on the yield of cantaloupe and broccoli for various germination practices and salt for water between (1.5 - 2.6 dS/m), and forecast salt allocation after a whole plant season. The soil is a sandy loam, and van Genuchten parameters were specified using Rosetta by entering the particle volume allocation and bulk density. Average initial soil profiles (saturated soil electrical conductivity ECe) to a deep of 30 cm was approximately 2.4 dS/m. The sink was used to calculate the water consumption by plant roots. The equation of Fickian-based convection–dispersion was used to described solute transport. Solute transport and water flow equations were solved by Galerkin linear finite elements numerically. Solutes were assumed that nonreactive and no net solubilization or dissolution. These assumptions allowed the salinity to be simulated based on the convection–dispersion equation for nonreactive solutes. The salts closing the roof may decrease the hydraulic conductivity for soil and cause extra runoff from the soil roof. Correlations show the model's capability to forecast ECe can be effective when the insert parameters like root allocation are noted. **(Kandelous and Simunek, 2010)** investigated simulated water movement in the soil from the subsurface emitter and estimated distance of the wetted area. A subsurface emitter irrigation system executed two groups of tests. One group tests were complete in the laboratory, and other group tests were executed in the field. The laboratory tests were executed on a lysimetric (200 ×100 ×1200 cm) full of a clay loam soil. Field tests were executed at the fieldwork on a clay loam soil, the depth of emitters were 5, 15, 25 cm in the soil like that in the laboratory. The method of Galerkin finite-element used HYDRUS-2D to solve the equation of water flow governing. The domain was rectangular (100 and 150 cm). A comparison of calculated and simulated data proved that HYDRUS-2D could be the best model to help in designing and control subsurface emitter irrigation systems to soils with various textures.

(Kahlaoui, et al., 2011) used subsurface and surface emitter irrigation with water salinity (6.57 dS/m) on three tomato types. The goal was to develop water irrigation management beneath saline conditions and assess the reactions of three tomato types to many irrigation methods. The test was defined using drips buried at 30 cm deep in the subsurface and on the surface of the soil. Irrigation system owns a significant influence on the salt of soil ECe, and it was obviously salt

higher in surface emitter than in subsurface emitter. The salts was increased because of raising the evaporation level close soil roof in the situation of the surface emitter. Salts can move down and extend to the root zone for the time of spread uniform of water and precipitation on the soil surface. This action may prevent nutrient uptake and water; therefore, it makes negative effects on yield and crop growth. **(Selim, et al., 2013 a)** investigated brackish irrigation water with salinity and soil water distribution under (surface drip irrigation DI). They used HYDRUS-2D simulation by supposing tomato plants with salinity soil. They found the influence of the irrigation system on moisture shape varies with the hydraulic soil characteristic, the influence of (initial soil moisture content θi) will vanish the next few days and don't have any important effect on distributions of soil salinity. In the sand, soil salinity was found near the emitter match to loamy sand and sandy loam. They used a 1.4 m drip line spacing and 35 cm drip spacing. When the first irrigation was ended, the wetted depth was smaller in sandy loam and loamy sand than in sand, because sand is distinguishing by less water-holding ability as compared to loamy sand and sandy loam. A region of high salinity in sand happened (0.4 – 0.55 m) away from emitter while it happened (0.50 – 0.65 m) for loamy sand and sandy loam, and it can be decreased by distributing mulch to reduce the evaporation rate.

The main objective of this research was to study the effect of subsurface drip irrigation with emitter and emitters located at variable depths in the Iraqi soils and of applying different water qualities of the water pattern distribution and salinity distribution in the soil profile and analyzing a two – dimensional water flow and solute distribution by using a numerical model (Hydrus-2D).

2. GOVERNING EQUATIONS

2.1. Water Equation

The Richards equation controlling water flow from a point source through saturated water stream in soils can be written in two-dimensional coordinates as follows **(Celia et al. 1990)**:

$$\frac{\partial \theta}{\partial t} = \frac{\partial}{\partial x}\left[K(h)\frac{\partial h}{\partial x}\right] + \frac{\partial}{\partial z}\left[K(h)\frac{\partial h}{\partial z}\right] + \frac{\partial K(h)}{\partial z} \quad (1)$$

θ = the soil volumetric water content (L^3. L^{-3}),

h = the soil water pressure head (L),

t = time (T),

$K(h)$ = the unsaturated hydraulic conductivity function (L / T),

x = the horizontal spatial coordinates (L), and

z = the vertical spatial coordinates (L).

2.2. Salt Equation

The advection-dispersion equation in a permeable medium and is given as **(Hillel, 1998)**:

$$\frac{\partial \theta c}{\partial t} = \frac{\partial}{\partial x}\left[Dxx\frac{\partial c}{\partial x} + Dxx\frac{\partial c}{\partial z} - qxc\right] + \frac{\partial}{\partial z}\left[Dzz\frac{\partial c}{\partial z} + Dzz\frac{\partial c}{\partial x} - qzc\right] \quad (2)$$

C = concentration of the salt in the fluid stage (ML^{-3}), t = time (T), x = the horizontal coordinates (L), z = the vertical coordinates (L), Dxx, Dzz = the dispersion coefficient (L^2T^{-1}), q = flux of the solution (LT^{-1}).

Hydraulic conductivity with water holding was used to simulated soil hydraulic parameters illustrate by the van Genuchten–Mualem linkage and describe by **(Mualem 1976; van Genuchten 1980)**:

$$\theta(h) = \begin{cases} \theta_r + \dfrac{(\theta_s - \theta_r)}{(1 + |\alpha\, h\,|^{n})^{m}} & h < 0 \\ \theta_s & h \geq 0 \end{cases} \quad (3)$$

$$K(h) = K_s S_e^{\,I} \left[1 - \left(1 - S_e^{\,1/m}\right)^{m}\right]^2 \quad (4)$$

$$m = 1 - \frac{1}{n} \quad (5)$$

$$S_e = \frac{\theta - \theta_r}{\theta_s - \theta_r} \quad (6)$$

θs = volumetric saturated water content (L^3L^{-3}), θr = volumetric residual water content (L^3L^{-3}), n = pore-size distribution index dimensionless, α = inverse of the air-entry value (L^{-1}),
Ks = saturated hydraulic conductivity (LT^{-1}), I = shape factor and Se = is the proportional saturation (dimensionless).

2.3. Domain and Boundary Conditions

The domain to whole scenarios was classified to be axisymmetric about a perpendicular pivot. The water flows from a subsurface emitter is two-dimensional axisymmetric, "half the flow domain required to be simulated in HYDRUS - 2D" **(Kandelous, et al., 2011; El-Nesr and Alazba, 2017)**. The single subsurface emitter was placed at the upper left of the domain. Three emitter depths were used in this study (10, 20, and 30) cm. The simulation was carried out on a rectangle domain in this research. The domain was 80 cm in width and 100 cm in depth. The domain was selected large enough to avoid interference in the water content of near emitters.
The boundary conditions considered in this research are: the top boundary of the domain was submitting to atmospheric state, while the down boundary became a free drain. The border at both perpendicular directions was specified as "no-flux". Emitters were executing in all status as half circles with a radius of 1 cm, situated on the left vertical boundary of the domain. The emitter was defining a "Variable Flux". **Fig. 1** shows the boundary conditions considered in this study.
The irrigation flux can be calculated in HYDRUS-2D as follows, (assuming irrigation flux must not exceed the saturated hydraulic conductivity) **(Al Shammary and Salim, 2016) and (Abid, (2019)**.

$$q = \frac{Q}{2\pi r d} \quad (7)$$

q = irrigation flux per unit area (L/T), Q = flow rate of emitter (L^3/T),

d = distance between emitter (L), and r = radius of emitter (L).

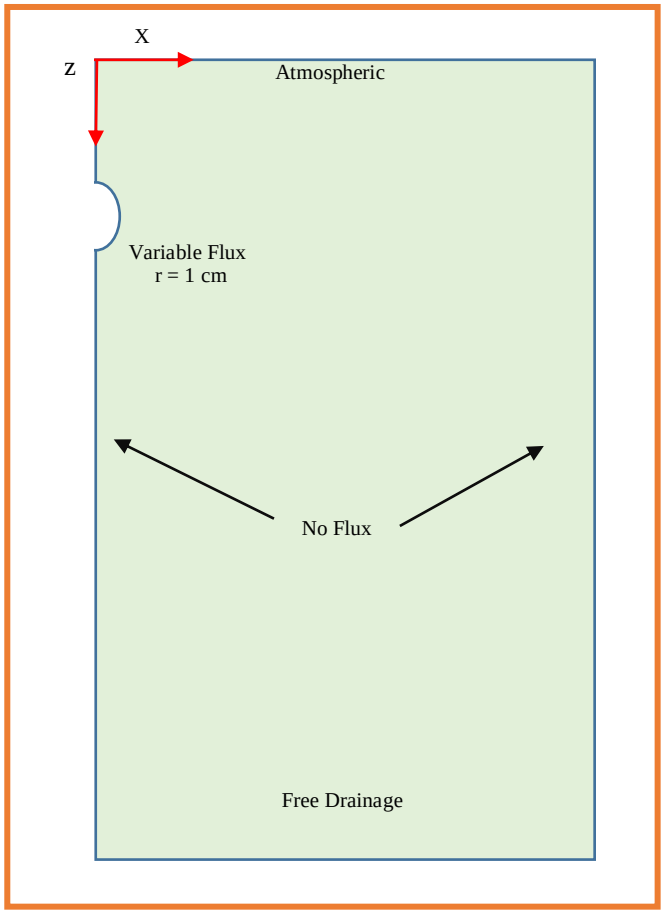

Figure 1. Schematic representation of boundary conditions

The soil is considered to be nil salinity at the beginning, and the salt concentration was put on through the emitter **(El-Nesr et al., 2013)**. Salt parameters demand are linear and lateral dispersivity (ƹL, ƹT, respectively). The ƹL was regulated equalize to a tenth of the profile deep while ƹT was set to equalize to 0.1 ƹL **(Anderson, 1984; Cote et al., 2001)**.

The boundary conditions performing salt as a third-type Cauchy boundary condition that prescribes the salt motion through determine irrigation periods.

To run the model, it needed an initial soil moisture content and the hydraulic parameters (Ks, θs, θr, α, n). These hydraulic parameters of the soil were assessed applying the Rosetta Lite software **(Schaap et al., 2001),** and it was involved in the HYDRUS-2D model.

Salinity for soil is a calculation of the concentration of whole dissoluble salts in water and soil, can ordinarily be presented as electrical conductivity (EC). The most commonly used EC units are deciSiemens per meter (dS/m).

Soil salt and water wetting patterns from a single subsurface emitter were simulated by using three types of Iraqi soil texture, classified as loam, sandy loam, and silty clay loam soil, respectively. **Table 1** illustrates the physical properties of the soils according to the laboratory test of the soil samples. Discharges of the emitter were shown in **Table 2,** were used in the simulation of the salt and water wetting patterns. In the simulation process, two initial volumetric soil moisture contents were used. The initial water content was limited between the field capacity and the welting point. The soil moisture content at field capacity, wilting point, and initial water content for Iraqi soil are shown in **Table 3.**

Table 1. Physical properties of Iraqi soils.

Soil texture	Ks (cm/hr)	θr ($cm^3.cm^{-3}$)	θs ($cm^3.cm^{-3}$)	α (cm^{-1})	n	Location	Reference
Sandy loam	5.65	0.061	0.371	0.027	1.41	Baghdad / Abu-Ghraib	Abid, 2019
Loam	2.1	0.044	0.393	0.013	1.46	Diwania	Abbass, 2018
Silty clay loam	4.7	0.088	0.466	0.009	1.48	Baghdad / Abu-Ghraib	Dawood, 2016

Table 2. Discharges of the emitter in (L/hr) for soil textures.

Soil texture	Q (*l/hr*)	
Sandy loam	0.75	1
Loam	0.3	0.4
Silty clay loam	0.5	0.75

Table 3. Values of initial soil moisture content and field capacity (F.C) and wilting point (W.P) for soil textures.

Soil texture	Initial volumetric moisture content ($cm^3.\ cm^{-3}$)		$\theta_{F.C}$ ($cm^3.\ cm^{-3}$)	$\theta_{W.P}$ ($cm^3.\ cm^{-3}$)
Sandy loam	0.09	0.098	0.124	0.075
Loam	0.18	0.2	0.260	0.132
Silty clay loam	0.26	0.3	0.348	0.189

3. STATISTICAL ANALYSIS

Statistical analysis was used to evaluate a relationship between the predicted results from HYDRUS-2D/3D software and those observed from the field. These parameters include root mean square error (RMSE), the optimal value approaches to zero, and the coefficient of correlation (R^2), which has the maximum at 1 when predicted values perfectly match the observed ones **(Shan, et al., 2011).**

$$RMSE = \sqrt{\frac{\sum_{i=1}^{n}(P_i - O_i)^2}{N}} \quad (8)$$

$$R^2 = 1 - \frac{\sum_{i=1}^{n}(P_i - O_i)^2}{\sum_{i=1}^{n}(O_i - \bar{O})^2} \quad (9)$$

N = is the total number of data points, *Pi* = is the predict data point, *Oi* = is the observed data and $\bar{O}$ = is the mean of observed.

4. RESULTS AND ANALYSIS

4.1. Validation of Results

The transient water and salt movement through three types of homogeneous Iraqi soil from a subsurface emitter were simulated. The simulation was done numerically using HYDRUS-2D model to study the distribution of soil salinity and its relationship with soil texture and characterize water and salinity distribution at different depth of subsurface emitter.

Equation (1) with the initial and boundary conditions as in **Fig. 1** and equation (2) were solved numerically using the finite element method with the HYDRUS-2D model. The accuracy of the predicted numerical results was validated by a comparison made between the predicted numerical results and the measured values of **(Shan and Wang, 2012)**. This comparison is illustrated in **Fig. 2** at a different distance from the intersection of overlap between two emitters. The numerical solution is seen to be in good agreement with field measurements.

4.2. Effect of Soil Types on Water Wetting Pattern

Fig. 3 shows water wetting pattern for a subsurface emitter in silty clay loam, loam and sandy loam soil, "initial soil moisture content" θi = 0.18 cm^3/cm^3, emitter discharge, Q = 0.4 L/h, EC= 8 dS/m and emitter depth =20 cm after end of simulation time 12 hr (irrigation time 3 hr).

The change in water wetting pattern distribution and initial soil moisture content was small. The wetting width and depth, in sandy loam soil, was bigger than in loam and silty clay loam soil, likewise in loam was bigger than in silty clay loam soil. The water wetting was spreading longitudinally and laterally, but the vertical spreading was more significant than the horizontal due to the gravity. In the finer-textured soils, there was less available air-filled pore space that reduced the infiltration capacity causing a considerable fraction of the applied water to move laterally, and this forced water to move far from the emitter.

Initial soil moisture content in silty clay loam was bigger than in loam and sandy loam soil, likewise in loam was bigger than in sandy loam soil. The reason was that because the characterized of the soils have lower hydraulic conductivity of sandy loam in addition to the higher water-holding capacity of sandy loam compared with loam and silty clay loam **(Abou Lila, et al., 2013).**

4.3. Effect of Soil Types on Salinity Wetting Pattern

Fig. 4 shows salt distribution for a subsurface emitter in sandy loam, loam and silty clay loam soil, θi = 0.18 cm^3/cm^3, Q= 0.4 L/h, EC= 8 dS/m and emitter depth =20 cm after end of simulation time (12 hr) (irrigation time 3 hr).

The change in salt pattern distribution and salt quantity was very small. The salt width, depth, and quantity in sandy loam soil were bigger than in loam and silty clay loam soil, likewise in loam was bigger than in silty clay loam soil, and that because characterized by the soils. The salt was spreading longitudinally and laterally, but the vertical spreading was larger than the horizontal by 49% due to the gravity**.**

4.4. Effect of Emitter Discharge (Q) on Salt and Wetted Soil Volume

Fig. 5 shows the salt pattern for a subsurface emitter in sandy loam for two θi (0.090 and 0.098 cm^3/cm^3) and two Q (0.75 and 1 L/h), EC= 8 dS/m and emitter depth =20 cm after the end of simulation time 3 hr (irrigation time 3 hr).

In all soil types, it was found that the wetted salt and wetting volume depended directly on the amount of irrigation water. Higher irrigation amounts initially produced higher salinity quantity and water content near the emitter. The larger lateral extension in sandy loam can be attributed to

less available air-filled pore space that decreases the infiltration capacity. Besides, the lower soil hydraulic conductivity limits the vertical movement of water and enhances the possibility of water moving laterally **(Selim, et al., 2013).**

4.5. Effect of Emitter Depth on Salt and Water Wetted Soil

Fig. 6 shows salt pattern for a subsurface emitter in silty clay loam soil, θi = 0.3 cm^3/cm^3, Q= 0.4 L/h, EC= 8 dS/m and emitter depth =10, 20 and 30 cm after end of simulation time 3 hr (irrigation time 3 hr).

The salt and water pattern reached the soil surface when the emitter depth is 10 cm, and that caused a rise in the losses of water by evaporation. The vertical spread of salt was larger than the lateral due to gravity; the salt quantity in a depth 10 cm is larger than 20 cm and 30 cm and has the bigger lateral spread. When the emitter depth was 30 cm, the salt and water wetting pattern may by penetrated to deep percolations. In the coarse-textured soil the perfect depth for emitter should be at deep depth (30 cm) and for medium-textured soil should be at a shallow depth (20 cm), noticing that the depth of the root of the plant to guarantee the transport of water straight to the roots **(Abid, 2019)**.

4.6. Effect of Initial Soil Moisture Content (θi) on Salt and Wetted Soil Volume

Fig. 7 shows salt pattern for a subsurface emitter in loam for two θi (0.18 and 0.2 cm^3/cm^3) and two Q (0.3 and 0.4 L/h), EC= 8 dS/m and emitter depth =20 cm after end of simulation time 3 hr (irrigation time 3 hr).

It was found that the soil moisture content decreased by 46% as the distance from the emitter increased. When θi decreased, the water wetting pattern and salinity pattern decrease too, but salinity quantity increase.

4.7. Effect of Irrigation Time on Salt and Water Wetted Soil

It was observed that when the duration of irrigation increases, the width and depth of salt and water pattern distribution increase largely, and almost all distributions pattern reaches the soil surface except when the emitter depth is 30 cm for two scenarios. It was noted that the maximum widths found when the emitter depth was 10 cm for two irrigation duration (12 and 24 hr), and the maximum depth found when emitter depth was 30 cm for two irrigation duration.

4.8. Effect of Salt on Crop Yield

In this simulation, the Cucumber plant was used with two values of EC= 8 and 4 dS/m in sandy loam soil. The results showed that irrigation with water has salt 8 dS/m, making the yield reduction =100%. A large amount of freshwater was needed to leach the accumulated salt in the soil, but when irrigating with water of 4 dS/m, the yield reduction became 25% to 50%, and little fresh water was used for leaching the salt.

5. CONCLUSIONS

1. The salt width, depth, and quantity in sandy loam soil have very little increase more than loam by 0.8%, 1.2%, and 0.3% and by 2.6%, 1.6%, and 0.55% from silty clay loam soil. Likewise, loam increased little more than silty clay loam soil by 1.8%, 0.5%, and 0.3%, as shown in **Fig. 4**.

2. The salt and water wetting are spreading longitudinally and laterally, but the vertical spreading was larger than the horizontal direction by 49%, for example, in sandy loam soil in **Fig. 3**. This is due to gravity action.
3. The wetted salt and water wetting volume are depended directly on the amount of irrigation water.
4. The soil moisture content was decreased by 46% as the distance from the emitter was increased, when θi was decreased, the water wetting pattern and salinity pattern decreased too. On the other side, the salinity quantity was increased by 2%, for example, in loam soil in **Fig. 7**.
5. The salt and water pattern reached the soil surface when the emitter depth is 10 cm, and that caused rise the losses of water by evaporation. When the emitter depth was 30 cm, the salt and water wetting pattern may be penetrated too deep percolations.
6. It was observed that when the duration of irrigation increases from 3 hr to 12 hr, the width and depth of salt and water pattern distribution increased largely. The width increased by 48% for water and 35% for salt, and the depth increased 47% for water and 35.6% for salt.
7. The plants which have salt tolerance and this rang intolerance can help to use the salty water for irrigation, which can produce a good yield with less freshwater is adding.

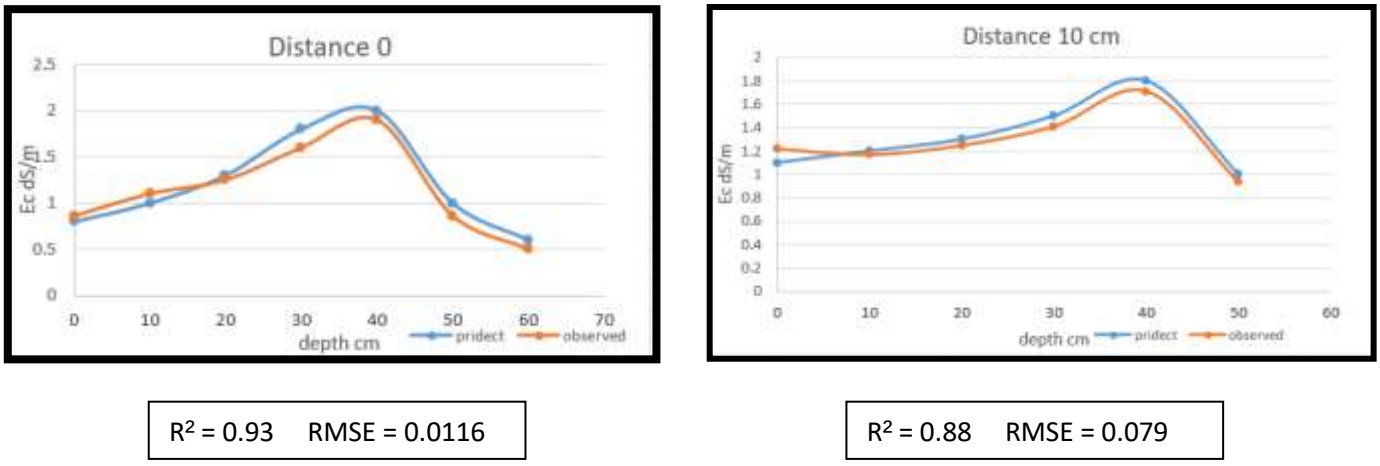

$R^2 = 0.93$ RMSE = 0.0116

$R^2 = 0.88$ RMSE = 0.079

Figure 2. validation between predict data from HYDRUS-2D and observed data.

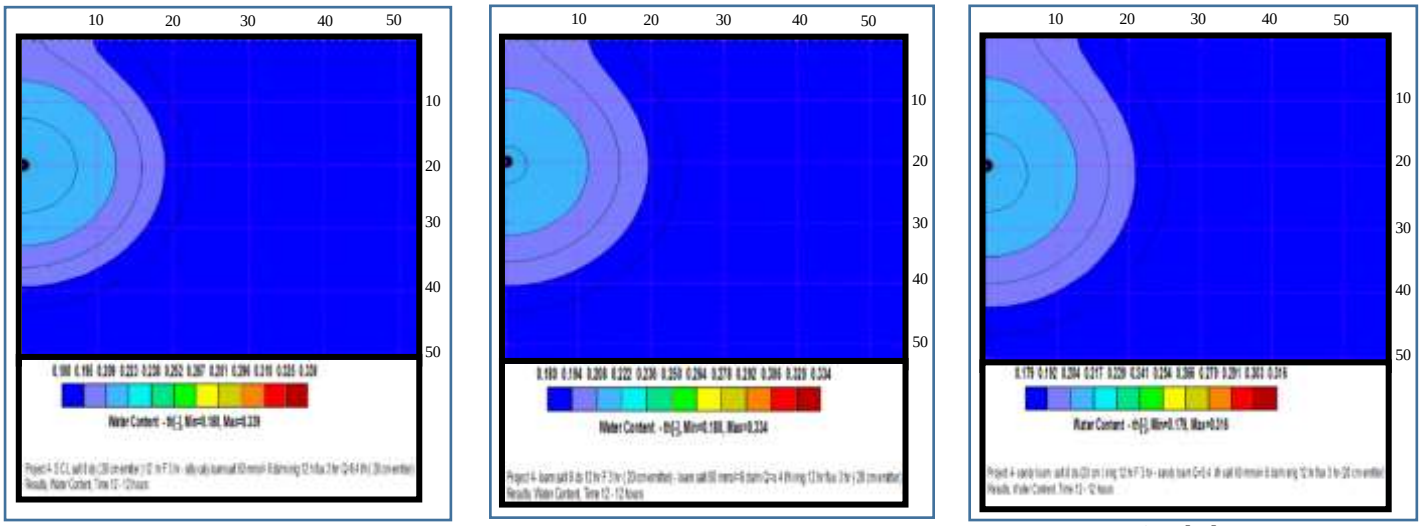

Figure 3. Simulation of water wetting pattern for a subsurface emitter in silty clay loam, loam and sandy loam soil, θi = 0.18 cm^3/cm^3, Q= 0.4 l/h, EC= 8 dS/m, emitter depth =20 cm after end of simulation time 12 hr (irrigation time 3 hr).

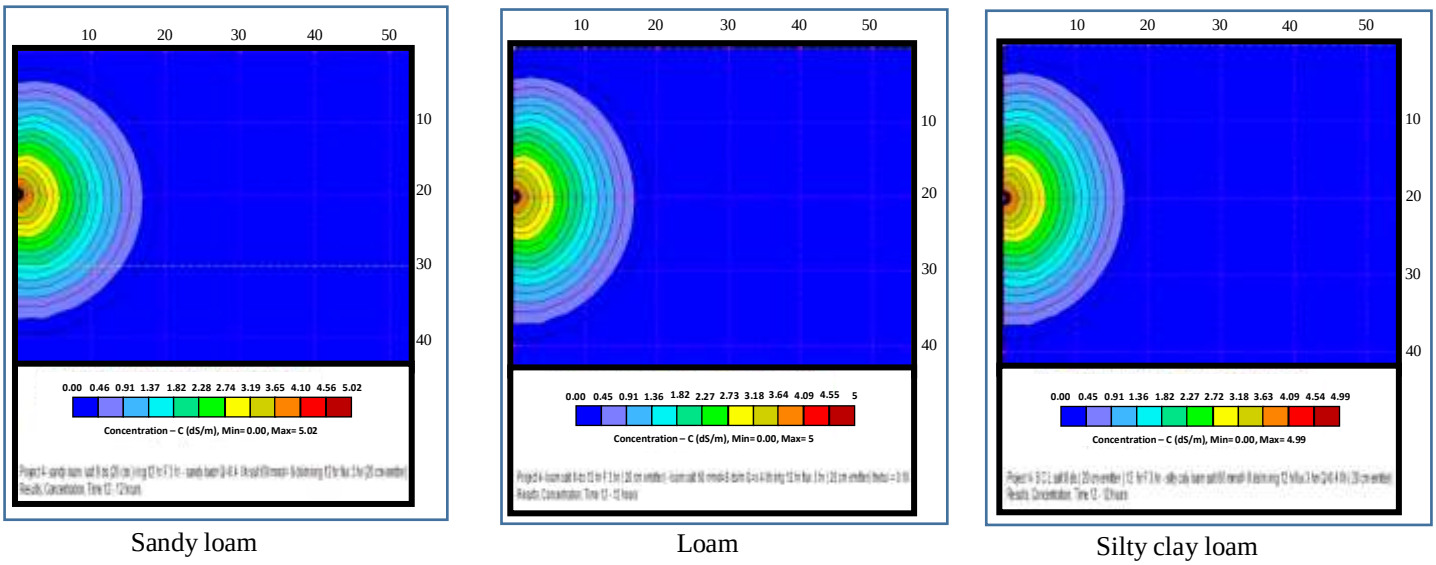

Figure 4. Simulation of salt pattern for a subsurface emitter in sandy loam, loam and silty clay loam soil, θi = 0.18 cm^3/cm^3, Q= 0.4 l/h, EC= 8 dS/m, emitter depth =20 cm after end of simulation time (12 hr) (irrigation time 3 hr).

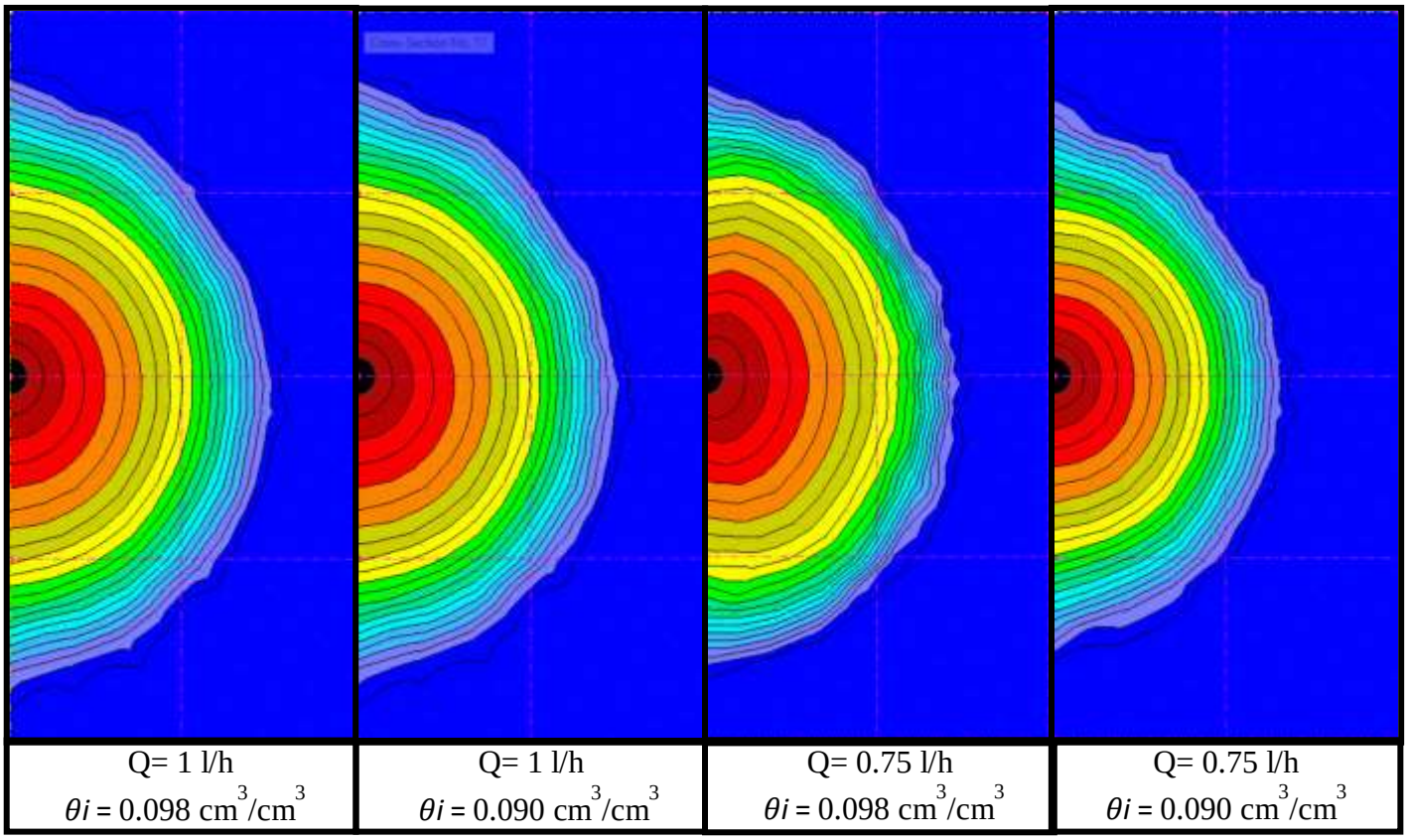

Figure 5. Simulation of salt pattern for a subsurface emitter in sandy loam for two θi and two Q, EC= 8 dS/m, emitter depth =20 cm after end of simulation time 3 hr (irrigation time 3 hr).

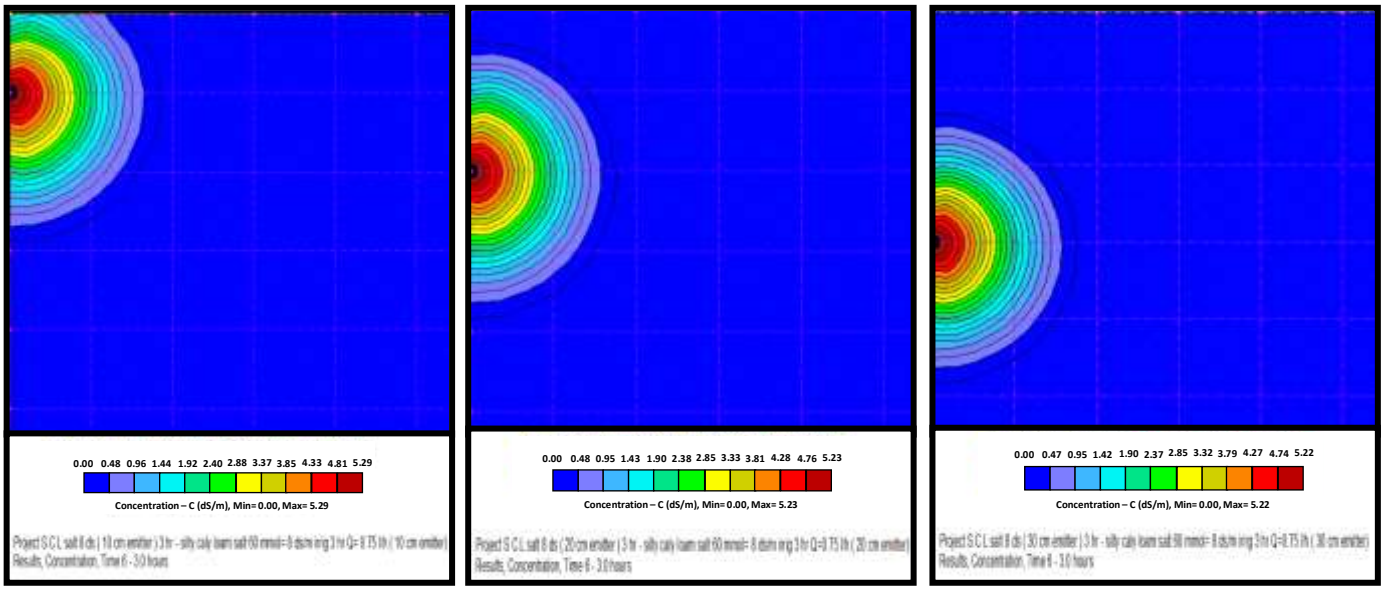

a - 10 cm emitter depth b - 20 cm emitter depth c - 30 cm emitter depth

Figure 6. Simulation of salt pattern for a subsurface emitter in silty clay loam soil, θi = 0.3 cm^3/cm^3, Q= 0.4 l/h, EC= 8 dS/m, emitter depth =10, 20 and 30 cm after end of simulation time 3 hr (irrigation time 3 hr).

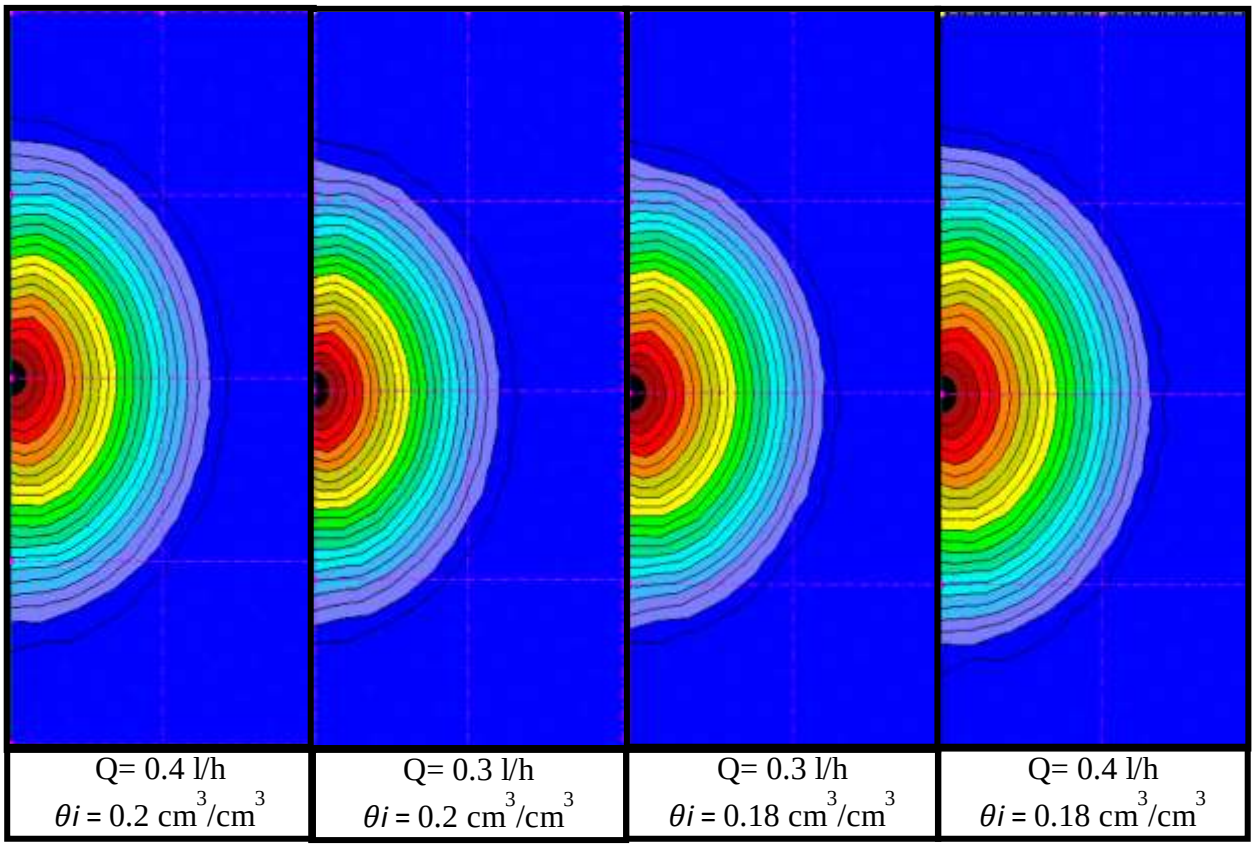

Figure 7. Simulation of salt pattern for a subsurface emitter in loam for two θi and two Q, EC= 8 dS/m, emitter depth =20 cm after end of simulation time 3 hr (irrigation time 3 hr).

5. REFERENCES

- Abbass, A. D., 2018. "Validation of Some Formulas for Obtaining Wetting Pattern under Surface Drip Irrigation". M.Sc. thesis, Department of Water Resources Engineering, College of Engineering, University of Baghdad, Baghdad, Iraq.
- Abid, H. N., 2019. "Predicting Wetting Patterns in Soil from a Single Subsurface Drip Irrigation System". University of Baghdad Journal of Engineering, September, Number 9, Volume 25.
- Abou Lila, T. S., Berndtsson, R., Persson, M., Somaida, M., El-Kiki, M., Hamed, Y., and Mirdan, A., 2013. "Numerical Evaluation of Subsurface Trickle Irrigation with Brackish Water". Irrigation Science, Vol. 31, No.2, pp. 1125–1137.
- Al Shammary, A. A., and Salim. S. B., 2016. "Measured and Predicted Wetting Patterns under Subsurface Drip Irrigation". International Journal of Science and Engineering Investigations. Vol.5, No.55, pp. 169-176.

- Anderson, MP., 1984. "Movement of contaminants in groundwater: groundwater transport-advection and dispersion. In Groundwater Contamination". Studies in Geophysics. National Academy: Washington, DC; 37–45.
- Celia, M.A., Bouloutas, E.T., Zarba, R.L., 1990. "A general mass conservation numerical solution for the unsaturated flow equation". Wiley Online Library, Water resources research.
- Cote, C.M., Bristow, K.L., Ford. E.J., Verburg, K., Keating, A.B., 2001. "Measurement of Water and Solute Movement in Large Undisturbed Soil Cores: Analysis of Macknade and Bundaderg Data". CSIRO Land and Water, Technical Report 07/01, Townsville, Australia.
- Dawood, I. A., 2016. "Movement of Irrigation Water from a Surface Emitter". University of Baghdad, Journal of Engineering Number 9, Volume 22, September 2016.
- El-Nesr, M. N., Alazba, A. A., and Šimunek, J., 2013. "HYDRUS Simulations of the Effects of Dual-Drip Subsurface Irrigation and a Physical Barrier on Water Movement and Solute Transport in Soils". Irrigation Science, Vol. 32, No.2, pp.111-125.
- El-Nesr, M.N., Alazba, A.A., 2017." Simulation of water distribution under surface dripper using artificial neural networks". Computers and Electronics in Agriculture 143, 90–99.
- Hillel, D., 1998. "Environmental soil physics". Academic Press, San Diego, CA. Hydrology, Vol. 251, pp. 163–176.
- Kahlaoui, B., Hachicha, M., Rejeb, S., Rejeb, M.N., Hanchi, B., and Misle, E., 2011. " Effects of Saline Water on Tomato Under Subsurface Drip Irrigation: Nutritional and Foliar Aspects". J. Soil Sci. Plant Nutr. 11 (1): 69 – 86.
- Kandelous, M. M., S˘imunek, J., 2010. "Numerical simulations of water movement in a subsurface drip irrigation system under field and laboratory conditions using HYDRUS-2D". Journal of Agricultural Water Management 97 1070-107 www.elsevier.com/locate/agwat .
- Kandelous, M.M., Simunek, J., Van Genuchten, M.Th., and Malek, K., 2011. "Soil water content distribution between two emitters of a subsurface drip irrigation system". Soil Sci. Soc. Am. J. 75:488–497.
- Mualem, Y., 1976. "A new model for predicting the hydraulic conductivity of unsaturated porous media". Water resources research, VOL. 12, NO. 3, 513–522.
- Roberts, T., Lazarovitch, N., Warrick, A. W., Thompson, T. L., 2009. "Modeling Salt Accumulation with Subsurface Drip Irrigation Using HYDRUS-2D". Soil Science Society of America, J. 73:233-240.
- Schaap, M. G., Leij, F. J., and van Genuchten, M. Th., 2001. "ROSETTA: A Computer Program for Estimating Soil Hydraulic Properties with Hierarchical Pedotransfer Functions". Journal of Hydrology 251, 163 – 176.
- Selim, T., Bouksila, F., Berndtsson, R., and Persson, M., 2013a. "Soil Water and Salinity Distribution under Different Treatments of Drip Irrigation". Soil Science Society of America, J. 77:1144–1156.

- Shan, Y. and Wang, Q., Wang, C., 2011." Simulated and measured soil wetting patterns for overlap zone under double points sources of drip irrigation". African Journal of Biotechnology Vol. 10(63), pp. 13744-13755.

- Shan, Y. and Wang, Q., 2012. Simulation of salinity distribution in the overlap zone with double-point-source drip irrigation using HYDRUS-3D ". Australian Journal of Crop Science, Vol. 6, No. 2, p: 238-247.

- Van Genuchten, M. Th., 1980. "A Closed-Form Equation for Predicting the Hydraulic Conductivity of Unsaturated Soils," Soil Science of America Journal, Vol. 44, pp. 892–898. Water resource Res 26:1483–1496.

NOMENCLATURE

θ_i= initial soil water content, (L^3/ L^3).
θ_r= residual water content, (L^3/ L^3).
θ_s= saturated water content, (L^3/ L^3).
t = time, (T).
Z= drip depth, (L).
K_s= saturated hydraulic conductivity, (L/T).
Q = emitter discharge, (L/T).
α = inverse of the air-entry value, (1/L).
n = pore size distribution index, dimensionless.
SDI = subsurface drip irrigation.
W = wetted width, (L).
D = wetted depth, (L).
d = distance between emitter (L) r = radius of emitter (L).
N = the total number of data points,
Pi = the predict data point,
Oi = the observed data,
$\bar{O}$ = the mean of observed data.
C = concentration of the salt in the fluid stage (ML^{-3}),
x = the horizontal coordinates (L),
z = the vertical coordinates (L),
Dxx, Dzz = the dispersion coefficient (L^2T^{-1}),